Proceedings of the World Congress on Engineering 2012 Vol III
WCE 2012, July 4 - 6, 2012, London, U.K.

Determination of the Reachable Workspace of 6-3 Stewart Platform Mechanism

Serdar Ay, O.Erguven Vatandas, and Abdurrahman Hacioglu

***Abstract*—In this paper, a novel geometrical methodology is introduced for determining the reachable workspace of 6-3 Stewart Platform Mechanism. The reachable workspace is one of the significant characteristic in determining the feasibility of utilizing SPM as a machine tool structure. The proposed method based on a geometrical approach is rather straightforward to evaluate the reachable workspace. Basically, it is based on determining attainable locations of three vertices for all possible leg configurations as all constraints dealing with legs and joints are taken into consideration.**

***Index Terms*—Kinematics, machine tool, workspace, Stewart Platform Mechanism.**

I. Introduction

Stewart Platform Mechanism (SPM) has been extensively utilized in many practical engineering applications ranging from CNC machining to satellite dish positioning since D.Stewart proposed SPM as a flight simulator [1]. Although it has recently received considerable attention from many researchers because of its advantages such as high structural rigidity, accuracy, force/torque capacity, there are major drawbacks such as complex forward kinematics and limited workspace. Therefore, researchers have focused on workspace of SPM and introduced many valuable studies for last three decades.

Merlet classified workspace determination methods into three groups, namely discretization methods, geometrical methods, and numerical methods [2]. Gossellin proposed the geometrical method for determining the constant orientation workspace of 6 degree of freedom parallel manipulator. [3]. Since SPM has also been utilized in CNC machining / 5-axis machining operations, some researchers have carried out some studies to achieve the knowledge of shape and size of workspaces and boundaries of SPMs [4]- [11].

Reachable workspace is a set which contains all the positions that can be achieved by a reference point on the end-effector [12] The knowledge of size and shape of workspace and boundary of SPM is of a great importance to locate the workpiece properly in order to avoid collisions between the cutting tool and the workpiece. Therefore, the reachable workspace is one of the significant characteristic in determining the feasibility of utilizing SPM as a machine tool structure.

The proposed method based on a geometrical approach is rather straightforward to evaluate the reachable workspace. Basically, it is based on determining attainable locations of three vertices for all possible leg configurations as all constraints dealing with legs and joints are taken into consideration.

The organization of this study is as follows. First, in Section II, the description of 6-3 SPM is presented. Secondly, in Section III, the proposed geometrical algorithm is introduced in detail. Thirdly, in Section IV, the implementation of the proposed method is presented. Finally, conclusions are made in Section V.

Serdar AY is with the Aeronautical and Astronautical Engineering Department, Turkish Air Force Academy, Yeşilyurt-İstanbul, Turkey (e-mail: say@ hho.edu.tr).
O.Erguven VATANDAŞ is with the Turkish Air Force Academy, Yeşilyurt-İstanbul, Turkey (e-mail: e.vatandas@hho.edu.tr).
Abdurrahman HACIOĞLU is with the Aeronautical and Astronautical Engineering Department, Turkish Air Force Academy, Yeşilyurt-İstanbul, Turkey (e-mail: hacioglu@ hho.edu.tr).

II. The description of 6-3 SPM

SPM consists of one rigid base and one rigid moving platform connected to each other through six extensible legs and spherical joints, as shown in Fig. 1. Depending on arrangement of legs, SPM is categorized into different types such as 6-3, 3-3, 6-6 etc.

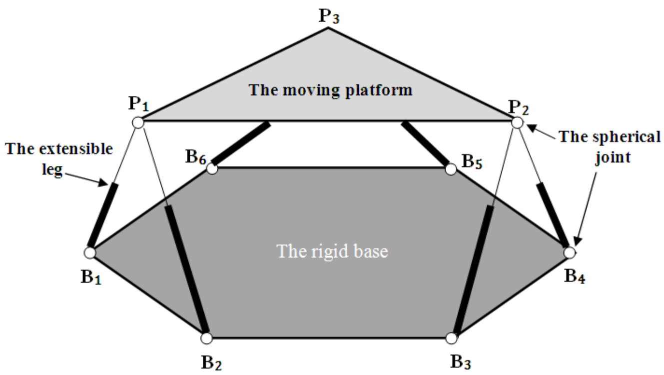

Fig. 1. 6-3 Stewart Platform Mechanism.

We consider a 6-3 SPM, the base and moving platform of which are equilateral hexagonal and triangle shaped respectively. Leg lengths are L_i varying between L_{imin} and L_{imax}, i=1, 6. The side length of fixed platform is L. The side lengths of movable platform are d_j, j=1, 3. Each pair of the six legs is attached to one vertex of moving platform. B_i and P_j are the centers of the joints located on the fixed and moving platforms, respectively. Geometric relations among

ISBN: 978-988-19252-2-0
ISSN: 2078-0958 (Print); ISSN: 2078-0966 (Online)

vertices P_1, P_2, P_3 and other parameters were presented by Nanua et al. [13].

III. The Proposed Methodology

The methodology consists of three steps. In each step, the position of one of the vertices is determined. The details of steps are presented in the following sections:

A. The Determination of Position of Vertex P_1

The coordinates (p_{1x}, p_{1y}, p_{1z}) of vertex P_1 in Fig. 3 are determined by varying lengths of L_1, L_2 and Φ_1 with respect to the constraints of L_1, L_2, and joints.

L_{bi} and r_j are the distances between B_i and O_j, and between P_j and O_j, respectively, as shown in Fig. 2.

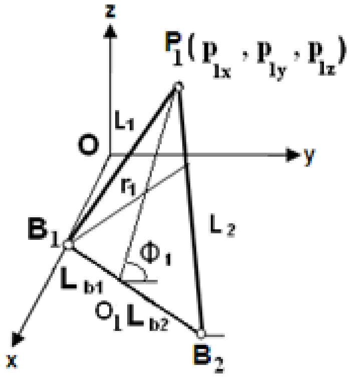

Fig. 2. The location of vertex P_1.

It is necessary to express L_{b1}, L_{b2} and r_1 for vertex P_1 in terms of leg lengths. These expressions include the following:

$$L_{b1} = \frac{L^2 + L_1^2 - L_2^2}{2L} \quad (1)$$

$$L_{b2} = L - L_{b1} \quad (2)$$

$$r_1 = \sqrt{L_1^2 - L_{b1}^2} \quad (3)$$

The coordinates (x_{01}, y_{01}) of O_1 are given by the following equations:

$$x_{01} = x_{b1} + L_{b1}\cos(\pi - \alpha_1) \quad (4)$$

$$y_{01} = y_{b1} + L_{b1}\sin(\pi - \alpha_1) \quad (5)$$

where (x_{b1}, y_{b1}) are the coordinates of B_1 and α_1 is the angle between x axis and O_1, as shown in Fig. 3.

The coordinates (p_{1x}, p_{1y}, p_{1z}) of vertex P_1 are given by the following equations:

$$p_{1x} = x_{O1} - r_1\cos\phi_1\sin(\pi - \alpha_1) \quad (6)$$

$$p_{1y} = y_{O1} + r_1\cos\phi_1\cos(\pi - \alpha_1) \quad (7)$$

$$p_{1z} = r_1\sin\phi_1 \quad (8)$$

where Φ_1 determined by considering the limitations of joints is the angle between the planes of x-y and the triangle $B_1P_1B_2$.

Varying L_1, L_2 and Φ_1 discretely with respect to the related constraints describes the entire achievable positions of the first vertex.

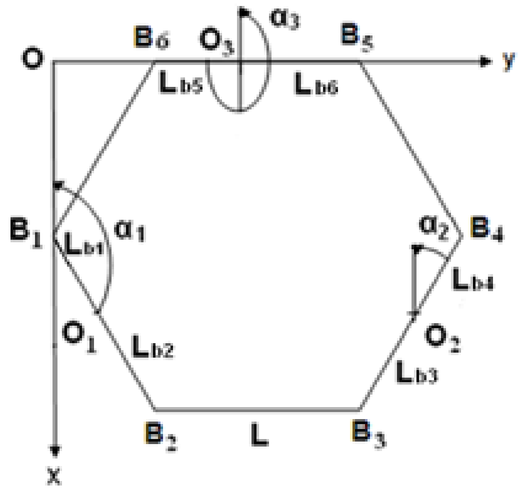

Fig. 3. Top view of the fixed base.

B. The Determination of Position of Vertex P_2

In this phase, the lengths of L_3 and L_4 are varied discretely with respect to the related constraints. The coordinates (p_{2x}, p_{2y}, p_{2z}) of vertex P_2 are determined by considering L_3, L_4, and the coordinates (p_{1x}, p_{1y}, p_{1z}) of vertex P_1 determined in previous phase.

In order to determine P_2 (p_{2x}, p_{2y}, p_{2z}) the geometrical relation between P_1 and P_2 is taken into account. Vertex P_2 may be located on the sphere centered at P_1 with radius d_1, as shown in Fig 4.

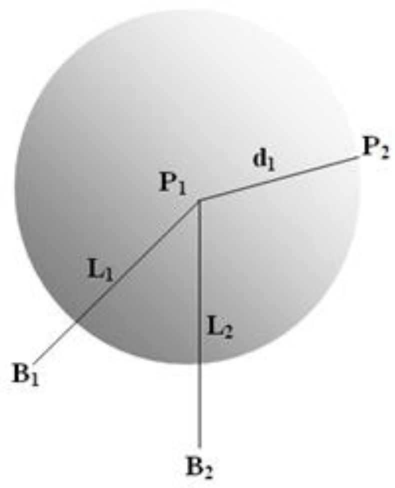

Fig. 4. The sphere centered at P_1 with d_1 radius.

Let t be the axis on x-y plane which is perpendicular to the line B_3B_{4a} and passes through O_2 as shown in Fig. 5. Varying lengths of L_3 and L_4 and keeping P_1 fixed, vertex P_2 moves in the circle centered at O_2 with radius r_2, which lies on t-z plane. In order to determine the coordinates (p_{2x}, p_{2y}, p_{2z}) of vertex P_2, it is necessary to figure out whether or not the sphere centered at P_1 and the circle centered at O_2 intersect.

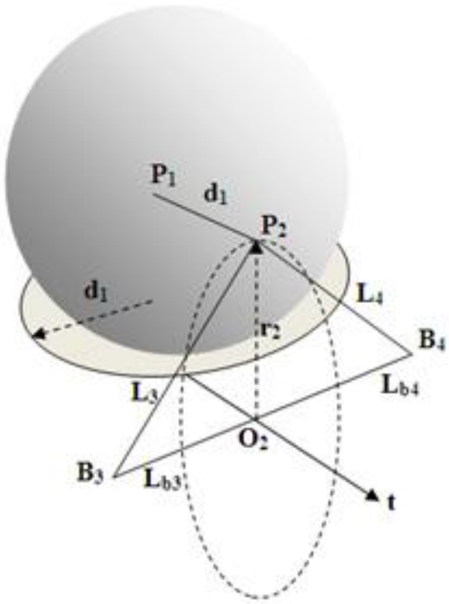

Fig. 5. The circle centered at O_2 with radius r_2.

This intersection may exist, providing that the intersection on *x-y* plane between the projection of the sphere and the axis *t* exists. The projection on *x-y* plane of the sphere is the circle centered P'_1 with radius d_1. The axis *t* can be defined as a line ($y=mx+k$) as shown in Fig.6.

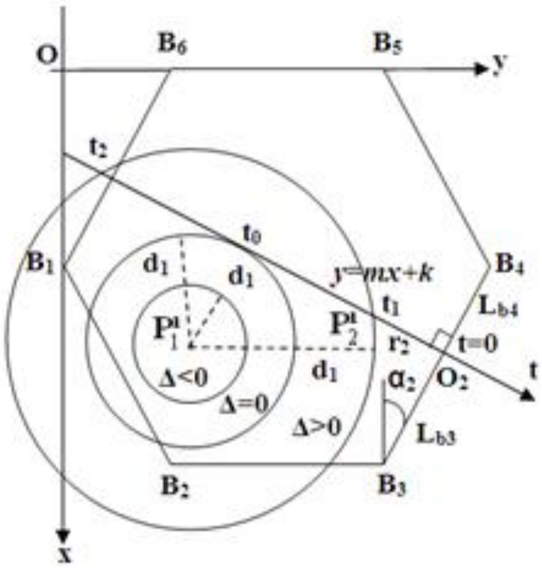

Fig. 6. The projections on x-y plane.

The circle with radius d_1 is expressed by the following equation:

$$\left(x-p_{1x}\right)^2+\left(y-p_{1y}\right)^2=d_1^2 \quad (9)$$

The following equation is written to define the intersection on *x-y* plane:

$$(x-p_{1x})^2+(mx+k-p_{1y})^2=d_1{}^2 \quad (10)$$

This quadratic equation possesses two reel roots in the case $\Delta>0$. These reel roots correspond to the point t_1 and t_2 enabling to calculate the radius of the circle located on the *t-z* plane which is the projection of the sphere centered at P_1. The radius of the circle is given by the following equation:

$$r=\frac{\left|t_2-t_1\right|}{2} \quad (11)$$

To determine P_2, an additional intersection on the *t-z* plane shown in Fig. 8 between the circle with radius *r* and the circle with radius r_2 must be existed. This intersection occurs when the following relation is satisfied:

$$\left|r-r_2\right|\le l\le r+r_2 \quad (12)$$

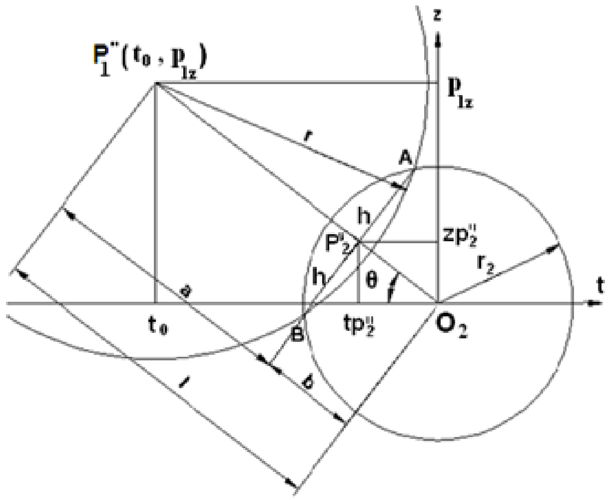

Fig. 7. The projections on *t-z* plane.

The radius r_2 of the circle centered at O_2 is given by the subsequent equation;

$$r_2=\sqrt{L_3^2-L_{b3}^2} \quad (13.a)$$

while the distance L_{b3} between B_3 and O_2 (see Fig. 3, 5 and 6) is defined as the following:

$$L_{b3}=\frac{L^2+L_3^2-L_4^2}{2L} \quad (13.b)$$

θ is the angle between the line $P_1{}''O_2$ and *t* axis. θ is given by the following equation:

$$\theta=a\tan\left(\left|\frac{p_{1z}}{t_0}\right|\right) \quad (14)$$

where

$$t_0=\frac{t_1+t_2}{2} \quad (15)$$

l, *a*,*b* and *h* are the distances, as shown in Fig. 7. These expressions include the following relations:

ISBN: 978-988-19252-2-0
ISSN: 2078-0958 (Print); ISSN: 2078-0966 (Online)

$$l = \sqrt{t_0^2 + P_{1z}^2} \qquad (16)$$

$$a = \frac{r^2 + l^2 - r_2^2}{2l} \qquad (17)$$

$$b = l - a \qquad (18)$$

$$h = \sqrt{r^2 - a^2} \qquad (19)$$

The projection on *t-z* plane of vertex P_2 (p_{2x}, p_{2y}, p_{2z}) is $P_2''(tp_2'', zp_2'')$ and tp_2'', zp_2'' are given by the following equations:

$$tp_2'' = b\cos(\theta) \qquad (20)$$

$$zp_2'' = b\sin(\theta) \qquad (21)$$

The coordinates of points *A* and *B* on *t-z* plane are

$$t_A = tp_2'' + h.\sin(\theta) \qquad (22)$$

$$z_A = tp_2'' + h.\cos(\theta) \qquad (23)$$

$$t_B = tp_2'' - h.\sin(\theta) \qquad (24)$$

$$z_B = tp_2'' - h.\cos(\theta) \qquad (25)$$

The coordinates (x_{03}, y_{03}) of O_2 are given by the following equations:

$$x_{02} = x_{b3} + L_{b3}\cos(\pi - \alpha_2) \qquad (26)$$

$$y_{02} = y_{b3} + L_{b3}\sin(\pi - \alpha_2) \qquad (27)$$

where (x_{b3}, y_{b3}) are the coordinates of B_3. The projections on *x-y* plane of points A and B can be written as

$$x_A = x_{O2} + t_A\sin(\alpha_2) \qquad (28)$$

$$y_A = y_{O2} + t_A\cos(\alpha_2) \qquad (29)$$

$$x_B = x_{O2} + t_B\sin(\alpha_2) \qquad (30)$$

$$y_B = y_{O2} + t_B\cos(\alpha_2) \qquad (31)$$

x_A , x_B and y_A , y_B are the solutions of the coordinates (p_{2x}) and (p_{2y}), respectively while z_A and z_B are the solutions of p_{2z}. Each solution of (p_{2x}, p_{2y}, p_{2z}) is accepted for the vertex P_2, if the associated constraints are satisfied.

C. The Determination of Position of Vertex P_3

Given the coordinates of vertices P_1 and P_2 calculated above, the geometric relations among P_1, P_2, and P_3 are utilized to figure out the coordinates (p_{3x}, p_{3y}, p_{3z}) of vertex P_3. For a fixed P_1 and P_2, P_3 moves in a circle centered at the point O' with the radius r_0, shown as in Fig. 8.

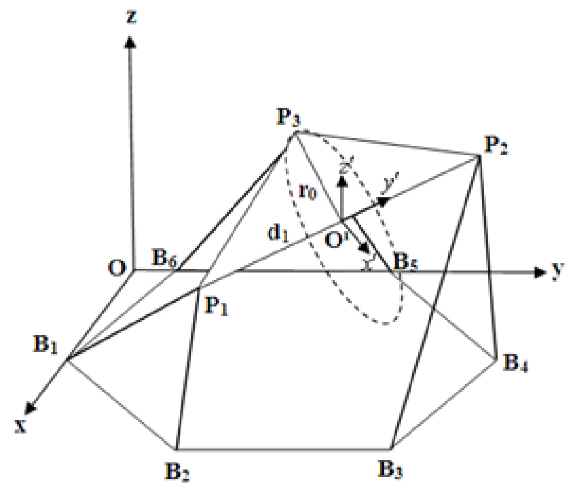

Fig. 8. The vertex *P3* moving in the circle with radius r_0.

The points on the circle with the radius r_0, where P_3 moves are utilized to determine the leg lengths of L_5 and L_6 through inverse kinematics. Providing that the determined leg lengths satisfy the constraints of the leg lengths and joints, the points are included to the solution set of the vertex P_3. In order to determine vertex P_3, the coordinate frame $O'(x'\ y'\ z')$ is defined. The origin of the coordinate frame $O'(x'\ y'\ z')$ is located at the center of the circle with the radius r_0, while y' axis passes through the line P_1P_2 and x' axis lying parallel to the *x-y* plane. P_3 moves along the arc corresponding to the angle φ (in radian). The radius r_0 is given by the following equation with the help of equilateral triangle relation:

$$r_0 = d_1 \frac{\sqrt{3}}{2} \qquad (32)$$

The vertex P_3 rotates about y' axis as shown in Fig. 9 and the equation of the circle with the radius r_0 relative to the coordinate frame $O'(x'y'z')$ can be rewritten as

$$(x')^2 + (z')^2 = r_0^2 \qquad (33)$$

where

$$x' = r_0\cos\varphi \qquad (34)$$

$$z' = r_0\sin\varphi \qquad (35)$$

The coordinates of the origin of $O'(x'y'z')$ are given by the following equation:

$$x_0' = \frac{(p_{1x} + p_{2x})}{2} \qquad (36)$$

$$y_0' = \frac{(p_{1y} + p_{2y})}{2} \qquad (37)$$

$$z_0' = \frac{(p_{1z} + p_{2z})}{2} \qquad (38)$$

The coordinates of the geometric center C (a_0, b_0, c_0) of the moving platform are given by following equations:

ISBN: 978-988-19252-2-0
ISSN: 2078-0958 (Print); ISSN: 2078-0966 (Online)

The coordinates of the geometric center C (a_0, b_0, c_0) of the moving platform are given by following equations:

$$x_0 = \frac{2x'_0 + p_{3x}}{3} \tag{39}$$

$$y_0 = \frac{2y'_0 + p_{3y}}{3} \tag{40}$$

$$z_0 = \frac{2z'_0 + p_{3z}}{3} \tag{41}$$

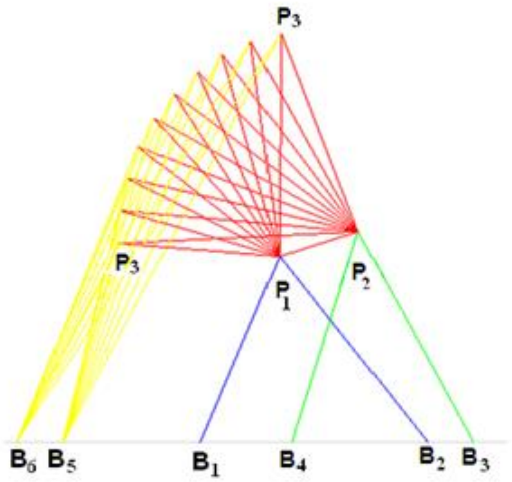

Fig. 9. The points reached by vertex P_3.

B_5 and B_6 as shown in Fig. 10 are the points on the fixed platform where L_5 and L_6 are connected, respectively. The coordinates of these points are transformed to the coordinate frame $O^t(x^t\ y^t\ z^t)$. To settle on P_3, the circle is split into $\Delta\theta$ intervals. Using inverse kinematics, the points satisfying all constraints correspond to P_3 (a_3, b_3, c_3).

Determined the coordinates of three vertices, the geometric center of the mobile platform is figured out. That the vertices P_2 and P_3 are evaluated for each achievable position of vertex P_1 results in the workspace.

IV. The Implimentation of the proposed Method

A 6-3 SPM with L=1 m, d_i=1 m, L_{min}=0.8 m, L_{max}=1.2 m is considered. The joint angle limitation varies between – 45^o and 45^o. The proposed algorithm results in the workspace in Fig. 10.

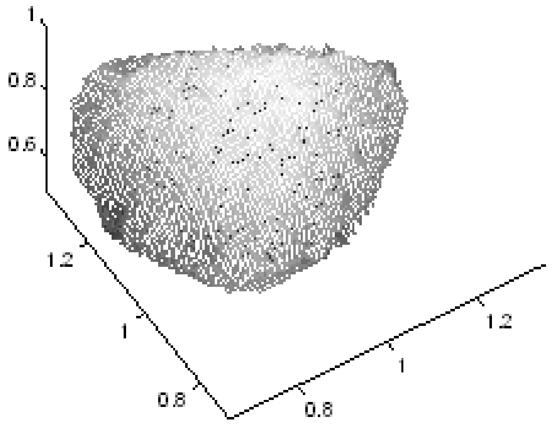

Fig. 10. The reachable workspace of 6-3 SPM.

V. Conclusions

The knowledge of the overall size and shape of workspace and boundary of SPM is of a great importance to locate the workpiece properly in order to avoid collisions between the workpiece and the cutting tool. Therefore, the reachable workspace is one of the significant characteristic in determining the feasibility of utilizing SPM as a machine tool structure. The proposed method based on a geometrical approach is rather straightforward to evaluate the reachable workspace.

Although the entire possible leg configurations are considered to achieve the workspace by using both the forward kinematics and inverse kinematics techniques, the proposed method does not require highly nonlinear algebraic equations with multiple solutions and time-consuming numerical analysis which needs good initial values and doesn't always converge at an expected point by means of all mechanical constraints.

References

[1] D.Stewart, "A platform with six degrees of freedom," Proc.Inst.Mech.Eng.vol.180, Pt1, No.1, 1965, pp. 371-386.
[2] J.P.Merlet,,*Parallel Robots*,Netherland, Springer, 2006.
[3] CM.Gosselin, "Determination of the workspace of 6-Dof parallel manipulators," ASME J.Mech.Des, 1990, pp. 112.
[4] I.Bonev and J.Ryu, " new approach to orientation workspace analysis of 6-DOF parallel manipulators," Mechanism and Machine Theory 36, 2001, pp. 15-28.
[5] Z.Wang, Z.Wang, W.Liu, and Y.Lei, "A study on workspace, boundary workspace analysis and workpiece positioning for parallel machine tools," Mechanism and Machine Theory 36, 2001, pp. 606-622.
[6] M.Terrier, A.Dugas, and J-Y Hascoet, "Qualification of parallel kinematics machines in high-speed milling on free form surfaces," International Journal of Machine Tools & Manufacture 44, 2004, pp. 865-877.
[7] T.C.Lee and M.H. Perng, "Analysis of simplified position and 5-DOF total orientation workspace of a hexapod mechanism," Mechanism and Machine Theory 42, 2007, pp. 1577-1600.
[8] T.C.Lee and M.H. Perng, "Analysis of simplified position and 5-DOF total orientation workspace of a hexapod mechanism," Mechanism and Machine Theory 42, 2007, pp. 1577-1600.
[9] Z.Wang, S.Ji, Y. Li, and Y.Wan, "A unified algorithm to determine the reachable and dexterous workspace of parallel manipulators," Robotics and Computer-Integrated Manufacturing 26, 2010, pp. 454-460.
[10] C.Brisan and A. Csiszar, "Compution and analysis of the workspace of a reconfigurable parallel robotic system," Mechanism and Machine Theory 46, 2011, pp. 1647-1668.
[11] V.T.Portman, V.S. Chapsky, and Y. Shneor, "Workspace of parallel kinematics machines with minimum stiffness limits: Collinear stiffness value based approach," Mechanism and Machine Theory 49, 2012, pp. 67-86
[12] X.Yang, H.Wang, C.Zhang, and K.Chen, "A method for mapping the boundaries of collosion-free reachable workspaces," Mechanism and Machine Theory 45, 2010, pp. 1024-1033.
[13] Nanua, K. J. Waldron, and V. Murthy, "Direct kinematic solution of a Stewart platform," IEEE Trans. Rob. Automation 6(4), 1990, pp.438–444.

ISBN: 978-988-19252-2-0
ISSN: 2078-0958 (Print); ISSN: 2078-0966 (Online)